

# New Insights into Nisin's Antibacterial Mechanism Revealed by Binding Studies with Synthetic Lipid II Analogues

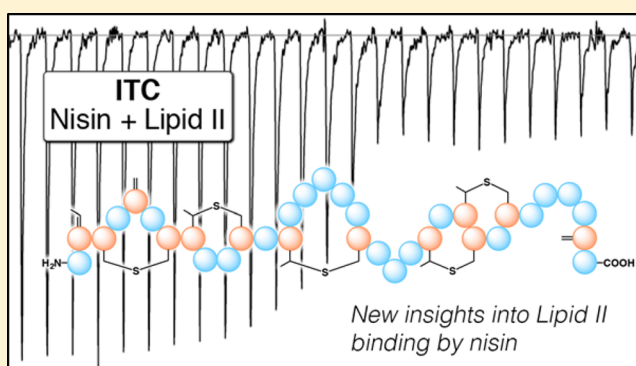
Peter 't Hart,<sup>†</sup> Sabine F. Oppedijk,<sup>‡</sup> Eefjan Breukink,<sup>‡</sup> and Nathaniel I. Martin<sup>\*,†</sup>

<sup>†</sup>Department of Medicinal Chemistry & Chemical Biology, Utrecht Institute for Pharmaceutical Sciences, Utrecht University, Universiteitsweg 99, 3584 CG Utrecht, The Netherlands

<sup>‡</sup>Membrane Biochemistry and Biophysics Group, Department of Chemistry, Utrecht University, Padualaan 8, 3584 CH Utrecht, The Netherlands

## S Supporting Information

**ABSTRACT:** Nisin is the preeminent lantibiotic, and to date its antibacterial mechanism has been investigated using a variety of techniques. While nisin's lipid II-mediated mode of action is well-established, a detailed analysis of the thermodynamic parameters governing this interaction has not been previously reported. We here describe an approach employing isothermal titration calorimetry to directly measure the affinity of nisin for lipid II and a number of synthetic lipid II precursors and analogues. Our measurements confirm the pyrophosphate unit of lipid II as the primary site of nisin binding and also indicate that the complete MurNAc moiety is required for a high-affinity interaction. Additionally, we find that while the pentapeptide unit of the lipid II molecule is not required for strong binding by nisin, it does play an important role in stabilizing the subsequently formed nisin–lipid II pore complex, albeit at an entropic cost. The anchoring of lipid II in a membrane environment was also found to play a significant role in enhancing nisin binding and is required in order to achieve a high-affinity interaction.



In order to address the growing threat posed by antimicrobial resistance, it is important that the mechanisms of action of new and existing antibiotics be clearly understood. The emergence of resistance against all major classes of clinically used antibiotics has led to an increased interest in less traditional antimicrobial agents, including antimicrobial peptides (AMPs) operating with unique modes of action. Among the best-studied of the AMPs is the bacteriocin nisin. Produced by strains of *Lactococcus lactis*, nisin is a member of the lanthipeptide family of AMPs because of the presence of (methyl)lanthionine rings and dehydro residues (Figure 1A). Nisin is widely active against Gram-positive bacteria, including drug-resistant pathogens, and while not suitable for use in humans, it is used widely in food preservation. As the preeminent lanthipeptide antibiotic (lantibiotic), nisin has received much attention, and its mode of action has been thoroughly studied.<sup>1–4</sup> A number of biochemical, biophysical, and NMR studies have shown that nisin interacts with the peptidoglycan precursor molecule lipid II. Upon binding to lipid II, nisin then goes on to form stable pores in the bacterial membrane, leading to rapid membrane depolarization and bacterial cell death. The lipid II molecule consists of a disaccharide core built from *N*-acetylglucosamine (GlcNAc) and *N*-acetylmuramic acid (MurNAc) wherein the MurNAc unit bears a pentapeptide at the 3 position. In addition, a C<sub>55</sub>

undecaprenol lipid is connected to the MurNAc anomeric center via a pyrophosphate linkage (Figure 1B). It is generally accepted that the pyrophosphate moiety of lipid II is recognized by the N-terminal part of nisin containing lanthionine rings A and B.<sup>5</sup> The remaining C-terminal region of the nisin peptide (rings C, D, and E) is then thought to insert into the bacterial membrane, leading to the formation of a pore complex with a nisin:lipid II stoichiometry of 8:4.<sup>6,7</sup> In addition to nisin, a number of other lantibiotics have also been found to contain homologous A/B ring systems, indicating that targeting of the pyrophosphate unit of lipid II is an antibacterial strategy employed by many organisms.<sup>1,8</sup> Such a strategy may in fact be particularly advantageous with respect to avoiding or delaying the development of resistance, as mutation of the pyrophosphate group does not appear to be readily feasible.<sup>9</sup>

The published solution-state NMR structure of the nisin–lipid II complex employed a soluble lipid II analogue bearing a shorter farnesyl lipid in place of the full C<sub>55</sub> undecaprenol tail.<sup>5</sup> While the structure thus obtained reveals the details of the interaction of the nisin A/B ring system with the lipid II pyrophosphate moiety, the factors governing pore formation

Received: October 29, 2015

Revised: December 10, 2015

Published: December 11, 2015

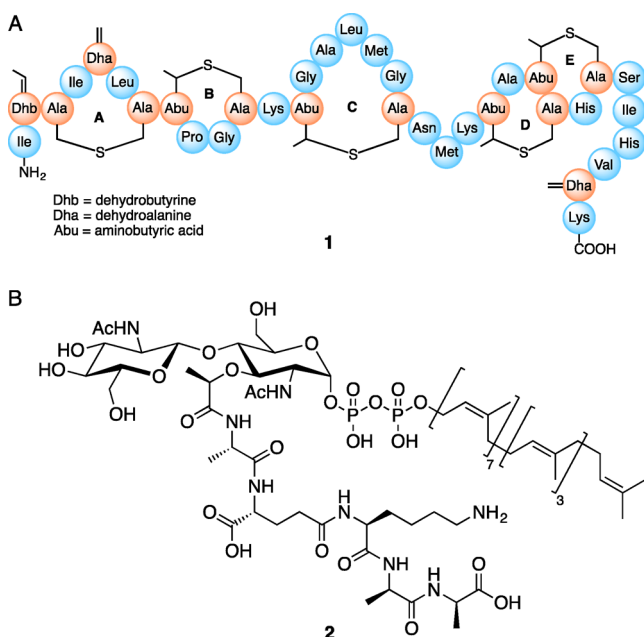


**Figure 1.** (A) Schematic structure of nisin. Amino acids in blue are natural amino acids. Amino acids in orange are unnatural amino acids. Dhb = dehydrobutyryne, Dha = dehydroalanine, Abu = aminobutyric acid. (B) Chemical structure of lipid II.

are not readily elucidated via such an approach. In this regard, a more commonly used technique for studying nisin-induced pore formation employs vesicles composed of 1,2-dioleoyl-*sn*-glycero-3-phosphocholine (DOPC) loaded with carboxyfluorescein.<sup>3</sup> When such vesicles are treated with nisin, pore formation can occur, resulting in dye leakage that can be detected as an increase in fluorescence signal. Using such an approach, Bonev and co-workers previously showed that nisin causes pore formation in vesicles that are supplemented with 1% lipid I or lipid II.<sup>10</sup> Conversely, nisin was found to be unable to induce pore formation in vesicles supplemented with undecaprenol pyrophosphate ( $C_{55}$ -PP) or monophosphate ( $C_{55}$ -P). They further studied the interaction of nisin with these vesicles using <sup>31</sup>P solid-state NMR spectroscopy and observed an interaction with lipid II, lipid I, and  $C_{55}$ -PP. In an alternative approach, the groups of Bendas and Sahl employed a quartz crystal microbalance approach to show that nisin has an enhanced affinity toward membranes containing lipid II.<sup>11</sup> In a more recent study, Schneider and co-workers used the same technique to measure the interaction of nisin with different undecaprenol-bound cell envelope precursors. They observed that the affinities of nisin for a variety of pyrophosphate-containing undecaprenol lipids were very similar, with  $K_d$  values in the 300–500 nM range.<sup>12</sup>

Another technique with the power to complement the approaches described above is isothermal titration calorimetry (ITC). ITC is one of the few techniques through which interactions between binding partners can be directly observed and quantified by measuring the change in heat that occurs upon binding, providing the full thermodynamic parameters of the binding interaction. Despite nisin's prominence as the best-studied lantibiotic, no comprehensive ITC study has yet been reported with the aim of examining its interaction with lipid II and related cell-wall precursors. While it is clear that the pyrophosphate unit of lipid II is essential for nisin binding, less is known about the roles played by the carbohydrate and

peptidic components in both the initial recognition by nisin and the subsequent formation of the nisin–lipid II pore complex. In this report, we describe the application of ITC to further study nisin's binding to lipid II as well as a variety of lipid II analogues. By doing so it is possible to identify the elements needed for high-affinity binding by nisin and to more fully elucidate the specific parameters that govern pore formation and stabilization.

## EXPERIMENTAL SECTION

**Isothermal Titration Calorimetry.** Large unilamellar vesicles containing 10 mM DOPC and 0.1 mM lipid of interest were prepared by suspending the dried lipid films in 50 mM Tris and 100 mM NaCl (pH 7.0). The solution was then extruded through 0.2  $\mu$ m pore filters 10 times. For  $C_{55}$ -PP, the vesicles were prepared using 10 mM DOPC and 0.5 mM  $C_{55}$ -PP. The nisin solution used was freshly prepared before every experiment in the same buffer system used to prepare the vesicles. All of the binding experiments were performed using a MicroCal-iTC200 microcalorimeter (Malvern). Each binding experiment consisted of 25 separate 1.5  $\mu$ L injections (following an initial injection of 0.5  $\mu$ L) delivered into the sample cell, which contained a 200  $\mu$ L volume of nisin at a concentration of 20  $\mu$ M (or 50  $\mu$ M for binding measurements with  $C_{55}$ -PP). The intervening time between each injection was 180 s, and all of the measurements were performed at 25  $^{\circ}$ C with the reference power set at “2”. The feedback mode/gain was set at “low” to obtain a better signal-to-noise ratio. For the titration with compound 8, a modified protocol was employed wherein compound 8 was dissolved at 800  $\mu$ M and nisin at 80  $\mu$ M. The binding measurements with compound 8 were performed by administering 19 separate injections of 2  $\mu$ L (following an initial injection of 0.5  $\mu$ L) at 180 s intervals into the sample cell containing the nisin solution.

All of the ITC binding experiments were conducted in triplicate and corrected by subtraction of a “blank” titration of the corresponding syringe solution into buffer. The binding data obtained were analyzed using the Origin 7.0 software supplied with the instrument.

**Dye Leakage Experiments.** Dye leakage assays were conducted as previously described,<sup>3</sup> with all of the experiments performed in triplicate. In short, carboxyfluorescein-loaded large unilamellar vesicles were prepared from 10 mM DOPC containing 0.2% lipid of interest. These vesicles were used at a concentration of 25  $\mu$ M in the cuvette, and the fluorescence was measured for 200 s. At approximately 40 s, nisin was added at a concentration of 10 nM, and after 140 s, Triton X-100 was added at a final concentration of 0.1%. The baseline signal ( $A_0$ ) was determined as the average of the first 40 s and the maximum signal ( $A_{max}$ ) as the average of the last 40 s. The value at 120 s ( $A_{measured}$ ) was used to calculate the percentage of dye leakage using the following formula:

$$\% \text{ leakage} = \frac{A_{measured} - A_0}{A_{max} - A_0} \times 100\%$$

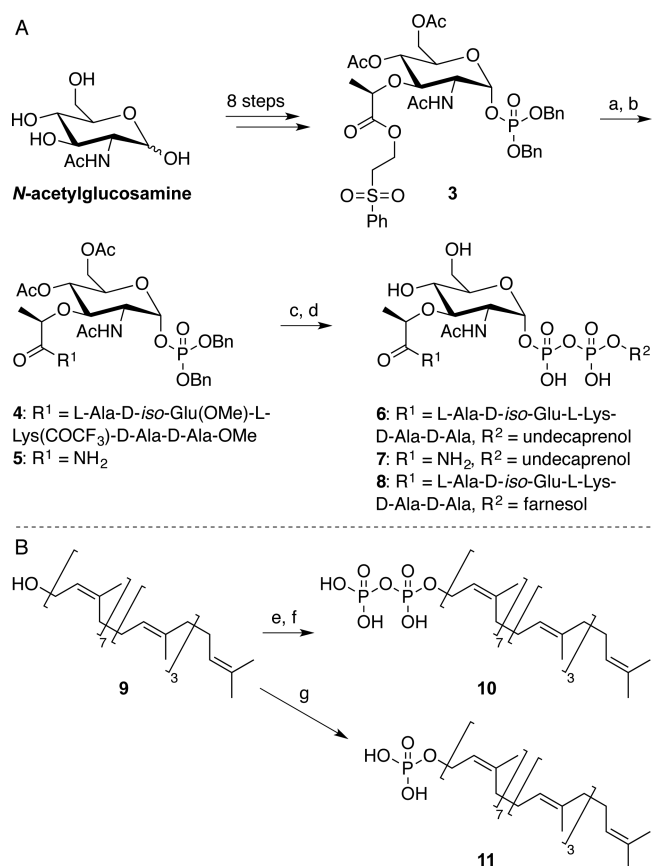
**Pore Stability Experiments.** Pore stability experiments were performed as previously described.<sup>3</sup> For these experiments, nisin was premixed with “empty” DOPC vesicles containing the lipid of interest. The cuvette was filled with carboxyfluorescein-loaded lipid II vesicles, and after 40 s the premixed vesicles were added. At  $t = 140$  s, Triton X-100 was added to obtain the 100% fluorescence signal. Each measure-

ment was performed in duplicate. For these experiments, the fluorescence signal obtained when using nisin alone (no empty vesicles added) was considered to be 100%.

## RESULTS AND DISCUSSION

For the purposes of the ITC investigations a variety of lipid II derivatives were prepared. Lipid II itself was synthesized via a previously described *in vitro* approach<sup>3</sup> using membrane preparations of *Micrococcus flavus* supplemented with C<sub>55</sub>-P, UDP-*N*-acetylmuramic acid pentapeptide, and UDP-GlcNAc. To assess the impact of omitting the GlcNAc moiety on nisin binding, lipid I was synthesized following a route similar to that developed by VanNieuwenhze and co-workers.<sup>13</sup> In addition, a lipid I analogue lacking the pentapeptide moiety was prepared in order to examine its role in nisin binding and pore formation. As illustrated in Scheme 1, the synthesis of lipid I and the other derivatives prepared proceeded via the common *N*-acetylmuramic acid derivative 3, which was prepared in eight steps from *N*-acetylglucosamine. Selective removal of the phenylsulfonyl ester protecting group in 3 followed by coupling with either the suitably protected pentapeptide<sup>13</sup> or ammonium chloride led to

**Scheme 1. Preparation of Lipid I, Lipid I Analogues, and C<sub>55</sub> Compounds for Use in ITC Binding Experiments<sup>a</sup>**



<sup>a</sup>Reagents and conditions: (A) (a) DBU, DCM, 2 h; (b) NH<sub>2</sub>-L-Ala-D-*iso*-Glu(OMe)-L-Lys(COCF<sub>3</sub>)-D-Ala-D-Ala-OMe or NH<sub>4</sub>Cl, BOP, DIPEA, DMF, 24 h; (c) H<sub>2</sub>, Pd/C, MeOH 1.5 h; (d) (i) carbonyldiimidazole, THF/DMF; (ii) MeOH; (iii) undecaprenol phosphate or farnesol phosphate, 1*H*-tetrazole, 4 days; (iv) NaOH, dioxane/H<sub>2</sub>O (1:1). (B) (e) CBr<sub>4</sub>, PPh<sub>3</sub>, DCM, 10 min; (f) tris(tetra-*n*-butylammonium) hydrogen pyrophosphate, CHCl<sub>3</sub>, 16 h; (g) tetra-*n*-butylammonium phosphate, CCl<sub>3</sub>CN.

the formation of intermediates 4 and 5, respectively. Removal of the benzyl protecting groups in 4 and 5 followed by activation of the free phosphate with carbonyldiimidazole and subsequent addition of C<sub>55</sub>-P led to the formation of the desired pyrophosphate-linked species. Once the pyrophosphate-forming step was deemed complete (as indicated by HPLC analysis), the crude intermediates were globally deprotected under basic conditions followed by HPLC purification to yield compounds 6 (lipid I) and 7 (lacking the pentapeptide). By means of the same general strategy, a water-soluble lipid I variant (8) was prepared by coupling the shorter C<sub>15</sub> farnesyl phosphate<sup>14</sup> in place of C<sub>55</sub>-P. In addition to the MurNAc-containing derivatives 6–8, C<sub>55</sub>-PP (10) was also prepared to allow an assessment of nisin binding to the simple lipid pyrophosphate. While C<sub>55</sub>-PP can be prepared via enzymatic synthesis,<sup>15</sup> we found a chemical synthesis starting from undecaprenol (9) to be quite feasible. To this end, 9 was first converted to the corresponding bromide by means of an Appel reaction. Subsequent displacement of the bromide by pyrophosphate, used as the tris(tetra-*n*-butylammonium) salt, then yielded C<sub>55</sub>-PP (10). C<sub>55</sub>-P (11) was prepared following a previously described procedure involving treatment of the alcohol with tetra-*n*-butylammonium phosphate and trichloroacetonitrile.<sup>14</sup>

The ITC experiments were performed using the undecaprenol-type lipids incorporated into DOPC vesicles at a final concentration of 0.1 mM. When solutions of these vesicle preparations were titrated into the ITC sample cell containing nisin at a concentration of 20 μM, it was possible to obtain high-quality binding curves for all of the pyrophosphate-containing lipid species (Figure 2). Of particular note is the observation that the order of addition is of key importance; attempts to titrate nisin into solutions of the lipid-containing vesicles failed to produce reliable ITC data. The results of the titrations performed are summarized in Table 1 and reveal low-nanomolar dissociation constants for all of the carbohydrate-based lipids evaluated (lipid II (2), lipid I (6), and compound 7). The K<sub>d</sub> of 14.6 nM obtained for nisin's binding to lipid II is in good agreement with the previously reported value of 50 nM determined from the binding behavior of radiolabeled nisin to DOPC vesicles containing 0.5 mol % lipid II.<sup>16</sup> In addition, the finding that nisin binds to both lipid II and lipid I with nearly the same affinity is in agreement with previously reported dye leakage studies indicating that the GlcNAc unit is not required for nisin binding.<sup>10</sup> The high-affinity binding of nisin measured with compound 7 (wherein the pentapeptide has been completely eliminated) further implicates the pyrophosphate diester moiety as the primary target for nisin binding. The ITC measurements also revealed nisin to have a relatively strong interaction with C<sub>55</sub>-PP (10), with an approximate 10-fold decrease in affinity compared with lipid II. This difference in binding may be explained by the presence of the extra negative charge in the pyrophosphate monoester moiety. In addition, titration of nisin with vesicles containing C<sub>55</sub>-P (11) and C<sub>55</sub>-OH (9) did not result in any observable binding (see SI Figures S14 and S15). These results are also in line with previous dye-leakage studies that found that both C<sub>55</sub>-P and C<sub>55</sub>-OH are unable to support nisin-induced pore formation.<sup>10</sup>

To probe the influence of the membrane environment in which the lipid II derivative is anchored, we also examined nisin binding to soluble lipid I analogue 8 in which the C<sub>55</sub> lipid was replaced by a farnesyl tail. When a vesicle-free solution of compound 8 was titrated into nisin, binding was observed (see



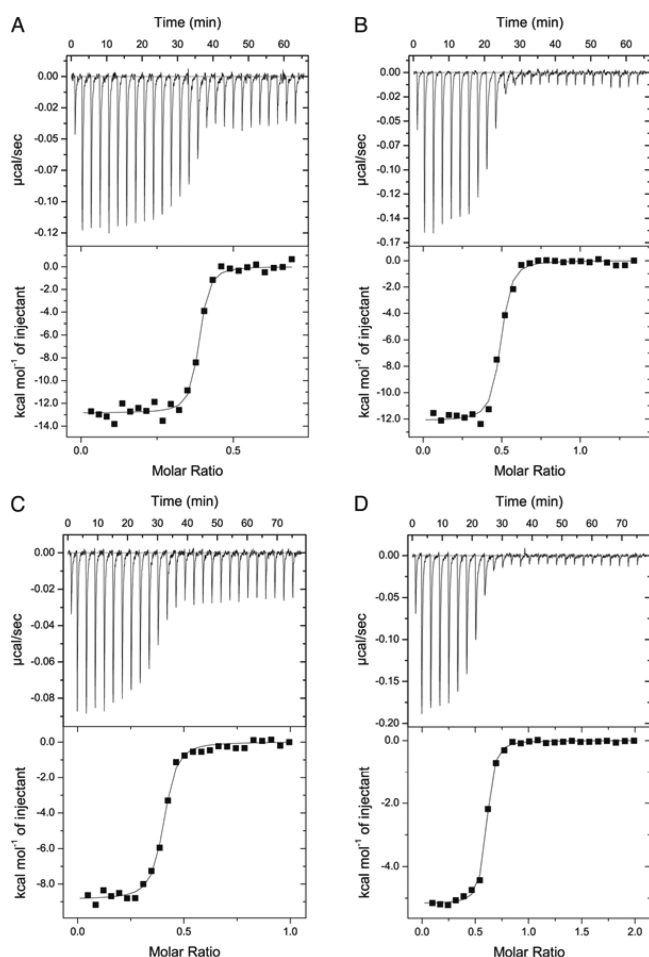


**Figure 2.** Representative isothermal titration measurements of DOPC vesicles containing (A) lipid II (2), (B) lipid I (6), (C) compound 7, or (D)  $C_{55}$ -PP (10) into nisin. For the measurements in (A–C), the lipid concentration was 100  $\mu\text{M}$ , and the concentration of nisin in the cell was 20  $\mu\text{M}$ . For the measurement in (D), the lipid concentration was 500  $\mu\text{M}$ , and the nisin concentration was 50  $\mu\text{M}$ . All of the vesicles were made with 10 mM DOPC.

SI Figure S16), albeit with a significant loss of affinity relative to the membrane-anchored lipid II and lipid I species. As indicated in Table 1, the  $K_d$  for nisin's interaction with compound 8 is approximately 100 times higher than that for lipid II. Also of note is the observation that nisin binding to compound 8 is an endothermic process and as such is completely entropy-driven. The large gain in entropy upon binding to 8 is likely due to the

displacement of organized water molecules that occurs upon formation of the nisin–8 complex, as is also evidenced by the visible aggregation and precipitation of the complex in aqueous solutions.

Interesting trends also emerge from the ITC data obtained for the various membrane-anchored  $C_{55}$  species. In moving from lipid II (2) and lipid I (6) to compound 7 and  $C_{55}$ -PP (10), a gradual decrease in the enthalpy of the nisin-binding interaction is observed (Table 1), suggesting the loss of stabilizing interactions (i.e., hydrogen bonds) and decreased pore stability. Another important finding is that for compound 7 and  $C_{55}$ -PP (10), both of which lack the pentapeptide, nisin binding is accompanied by a favorable gain in entropy compared with binding to lipid II (2) and lipid I (6), where binding comes at an entropic cost. This indicates that the pentapeptide experiences restricted motility within the nisin pore complex, leading to a high entropic penalty when it transitions from the free form into a pore complex. Removing the pentapeptide relieves this penalty.

The ITC experiments here described provide new insights into the structural requirements for high-affinity binding of lipid II by nisin. To correlate these findings with those elements of lipid II that are also required for nisin-induced pore formation, we next performed a series of dye leakage experiments with those lipid II derivatives that displayed the strongest nisin binding. To this end, we prepared a series of carboxyfluorescein-loaded DOPC vesicles containing the different  $C_{55}$  species and evaluated nisin's ability to induce pore formation as evidenced by dye leakage.<sup>3</sup> As illustrated in Figure 3A, the

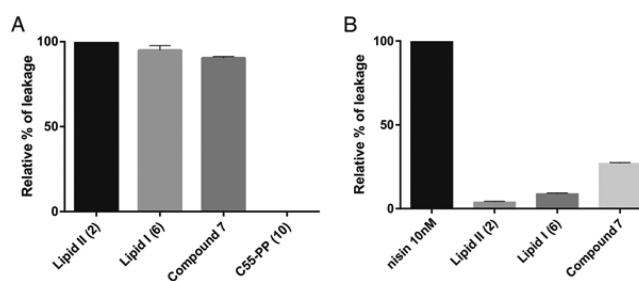


**Figure 3.** (A) Carboxyfluorescein (CF) leakage from DOPC vesicles upon addition of 10 nM nisin. (B) Leakage of CF from lipid II vesicles after addition of nisin-treated “empty” vesicles prepared with the indicated  $C_{55}$  compounds. The 100% leakage level corresponds to the value obtained upon treatment of lipid II-containing vesicles with nisin (black bar).

**Table 1. Thermodynamic Binding Parameters of Nisin and Various Lipid II and I Analogues Obtained by ITC Experiments<sup>a</sup>**

compound	$K_d$ (nM)	$\Delta H$ (kJ mol <sup>-1</sup> )	$\Delta S$ (J K <sup>-1</sup> mol <sup>-1</sup> )	$\Delta G$ (kJ mol <sup>-1</sup> )
lipid II (2) <sup>b</sup>	14.6 ± 3.8	-51.2 ± 2.3	-21.9 ± 8.0	-44.7 ± 0.6
lipid I (6) <sup>b</sup>	34.1 ± 8.2	-49.8 ± 0.8	-24.1 ± 3.3	-42.6 ± 0.6
7 <sup>b</sup>	25.7 ± 7.0	-35.1 ± 1.1	27.6 ± 4.4	-43.3 ± 0.7
$C_{55}$ -PP (10) <sup>c</sup>	132.6 ± 29.7	-21.7 ± 0.3	59.0 ± 2.1	-39.2 ± 0.6
$C_{55}$ -P (11) <sup>b</sup>	n.b. <sup>e</sup>	–	–	–
$C_{55}$ -OH (9) <sup>b</sup>	n.b. <sup>e</sup>	–	–	–
8 <sup>d</sup>	(1.2 ± 0.3) × 10 <sup>3</sup>	16.8 ± 1.2	169.9 ± 4.7	-33.9 ± 0.6

<sup>a</sup>Each data point is the average of three independent experiments (mean ± SE). Estimation of the errors in the thermodynamic parameters was done by Monte Carlo simulations using the standard error (SE) of each individual measurement. Full details of the ITC experiments are given in the Supporting Information. <sup>b</sup>Sample in syringe: 10 mM DOPC and 0.1 mM lipid. Sample in cell: 20  $\mu\text{M}$  nisin. <sup>c</sup>Sample in syringe: 10 mM DOPC and 0.5 mM lipid. Sample in cell: 50  $\mu\text{M}$  nisin. <sup>d</sup>Sample in syringe: 0.8 mM lipid, Sample in cell: 80  $\mu\text{M}$  nisin. <sup>e</sup>n.b. = no binding.

addition of nisin to vesicles containing lipid II, lipid I, or compound 7 resulted in similar levels of dye leakage. By comparison, and in agreement with previous reports,<sup>10</sup> nisin does not cause pore formation in vesicles containing C<sub>55</sub>-PP. The measured K<sub>d</sub> of 133 nM for binding of nisin to C<sub>55</sub>-PP does, however, appear to support the hypothesis that aside from targeting lipid II, nisin also inhibits bacterial growth by sequestration of C<sub>55</sub>-PP.<sup>10</sup> Also of note is the observation that compound 7, despite lacking the pentapeptide, is still able to support the formation of a viable pore complex with nisin. It was previously proposed that the MurNAc-pentapeptide motif was critical for pore formation,<sup>10</sup> but our data indicate that the MurNAc unit itself is largely sufficient. Following up on this finding, we next evaluated the stability of the pore complexes formed between nisin and lipid II, lipid I, or compound 7. The stabilities of the various pore complexes were examined by preincubating nisin with “empty” (no carboxyfluorescein) DOPC vesicles containing the various C<sub>55</sub> lipid species. The stability of the pore complexes formed in the empty vesicles was then assessed by adding carboxyfluorescein-loaded, lipid II-containing vesicles. The ability of nisin to dissociate from the initially formed pore complex in the empty vesicles is readily observed, as any free nisin rapidly rebinds to the carboxyfluorescein-loaded, lipid II-containing vesicles, resulting in dye leakage.<sup>3</sup> The results of the pore stability study (Figure 3B) show that the nisin-lipid II pore complex is quite stable, as reflected by the low level of leakage detected (<5%), while the pore complex formed with lipid I is slightly less stable (9% leakage). By comparison, the complex formed between nisin and compound 7 is significantly destabilized, as indicated by the >25% leakage observed, in line with our ITC results. Taken together, these findings suggest that while the pentapeptide unit is not required for strong binding by nisin and pore formation, it does play a role in stabilizing the nisin-lipid II pore complex.

## CONCLUSION

We have performed a comprehensive ITC-based investigation of the binding of nisin to its bacterial target molecule, lipid II. To date, a limited number of binding studies with other lantibiotics and lipid II have also been described.<sup>17–19</sup> Aside from these, ITC methods have also been applied to study the interaction of the polymyxin AMPs with their target molecule lipid A, the endotoxic component of the lipopolysaccharide characteristic of Gram-negative bacteria.<sup>20–22</sup> The present study is the first of its kind employing ITC as a means of characterizing nisin's interaction with lipid II. The ITC approach reveals subtle differences in the affinities of nisin for lipid II and derivatives lacking various structural features. The pyrophosphate moiety of lipid II was confirmed as the primary site of nisin binding, and new insights into the entropic features that accompany formation of the nisin pore complex were also revealed. Importantly, the ITC approaches here described are also expected to be of value in characterizing the modes of action of other antibiotics that target lipid II and related bacterial cell-wall precursors.

## ASSOCIATED CONTENT

### Supporting Information

The Supporting Information is available free of charge on the ACS Publications website at DOI: 10.1021/acs.biochem.5b01173.

Synthetic procedures and analytical data for all new compounds, including characterization data, NMR spectra, and analytical RP-HPLC traces; supporting figures for ITC binding studies as well as dye-leakage and pore stability assays (PDF)

## AUTHOR INFORMATION

### Corresponding Author

\*E-mail: n.i.martin@uu.nl.

### Funding

Financial support was provided by Utrecht University and The Netherlands Organization for Scientific Research (VIDI grant to N.I.M.).

### Notes

The authors declare no competing financial interest.

## ACKNOWLEDGMENTS

Sing Lau is kindly acknowledged for aiding in the chemical synthesis of compound 7. We thank Johan Kemmink for recording 2D NMR spectra and assistance with the analysis of ITC data. Javier Sastre Torano is also kindly acknowledged for providing HRMS analysis.

## REFERENCES

- (1) Breukink, E., and de Kruijff, B. (2006) Lipid II as a target for antibiotics. *Nat. Rev. Drug Discovery* 5, 321–332.
- (2) Bierbaum, G., and Sahl, H.-G. (2009) Lantibiotics: mode of action, biosynthesis and bioengineering. *Curr. Pharm. Biotechnol.* 10, 2–18.
- (3) Breukink, E., van Heusden, H. E., Vollmerhaus, P. J., Swiezewska, E., Brunner, L., Walker, S., Heck, A. J. R., and de Kruijff, B. (2003) Lipid II is an intrinsic component of the pore induced by nisin in bacterial membranes. *J. Biol. Chem.* 278, 19898–19903.
- (4) Breukink, E., Wiedemann, I., Van Kraaij, C., Kuipers, O. P., Sahl, H.-G., and de Kruijff, B. (1999) Use of the cell wall precursor lipid II by a pore-forming peptide antibiotic. *Science* 286, 2361–2364.
- (5) Hsu, S.-T. D., Breukink, E., Tischenko, E., Lutters, M. A. G., de Kruijff, B., Kaptein, R., Bonvin, A. M. J. J., and van Nuland, N. A. J. (2004) The nisin-lipid II complex reveals a pyrophosphate cage that provides a blueprint for novel antibiotics. *Nat. Struct. Mol. Biol.* 11, 963–967.
- (6) Breukink, E., Van Kraaij, C., Demel, R. A., Siezen, R. J., Kuipers, O. P., and de Kruijff, B. (1997) The C-terminal region of nisin is responsible for the initial interaction of nisin with the target membrane. *Biochemistry* 36, 6968–6976.
- (7) Brötz, H., Josten, M., Wiedemann, I., Schneider, U., Götz, F., Bierbaum, G., and Sahl, H.-G. (1998) Role of lipid-bound peptidoglycan precursors in the formation of pores by nisin, epidermin and other lantibiotics. *Mol. Microbiol.* 30, 317–327.
- (8) Willey, J. M., and van der Donk, W. A. (2007) Lantibiotics: peptides of diverse structure and function. *Annu. Rev. Microbiol.* 61, 477–501.
- (9) Zhou, H., Fang, J., Tian, Y., and Lu, X. Y. (2014) Mechanisms of nisin resistance in Gram-positive bacteria. *Ann. Microbiol.* 64, 413–420.
- (10) Bonev, B. B., Breukink, E., Swiezewska, E., de Kruijff, B., and Watts, A. (2004) Targeting extracellular pyrophosphates underpins the high selectivity of nisin. *FASEB J.* 18, 1862–1869.
- (11) Christ, K., Wiedemann, I., Bakowsky, U., Sahl, H.-G., and Bendas, G. (2007) The role of lipid II in membrane binding of and pore formation by nisin analyzed by two combined biosensor techniques. *Biochim. Biophys. Acta, Biomembr.* 1768, 694–704.
- (12) Müller, A., Ulm, H., Reder-Christ, K., Sahl, H.-G., and Schneider, T. (2012) Interaction of type A lantibiotics with undecaprenol-bound cell envelope precursors. *Microb. Drug Resist.* 18, 261–270.

(13) VanNieuwenhze, M. S., Mauldin, S. C., Zia-Ebrahimi, M. S., Aikins, J. A., and Blaszcak, L. C. (2001) The total synthesis of lipid I. *J. Am. Chem. Soc.* 123, 6983–6988.

(14) Danilov, L. L., Druzhinina, T. N., Kalinchuk, N. A., Maltsev, S. D., and Shibaev, V. N. (1989) Polyprenyl phosphates: synthesis and structure-activity relationship for a biosynthetic system of *Salmonella anatum* O-specific polysaccharide. *Chem. Phys. Lipids* 51, 191–203.

(15) El Ghachi, M., Bouhss, A., Blanot, D., and Mengin-Lecreux, D. (2004) The bacA gene of *Escherichia coli* encodes an undecaprenyl pyrophosphate phosphatase activity. *J. Biol. Chem.* 279, 30106–30113.

(16) Wiedemann, I., Breukink, E., van Kraaij, C., Kuipers, O. P., Bierbaum, G., de Kruijff, B., and Sahl, H.-G. (2001) Specific binding of nisin to the peptidoglycan precursor lipid II combines pore formation and inhibition of cell wall biosynthesis for potent antibiotic activity. *J. Biol. Chem.* 276, 1772–1779.

(17) Al-Kaddah, S., Reder-Christ, K., Klocek, G., Wiedemann, I., Brunschweiler, M., and Bendas, G. (2010) Analysis of membrane interactions of antibiotic peptides using ITC and biosensor measurements. *Biophys. Chem.* 152, 145–152.

(18) Paiva, A. D., Breukink, E., and Mantovani, H. C. (2011) Role of lipid II and membrane thickness in the mechanism of action of the lantibiotic bovicin HCS. *Antimicrob. Agents Chemother.* 55, 5284–5293.

(19) Islam, M. R., Nishie, M., Nagao, J., Zendo, T., Keller, S., Nakayama, J., Kohda, D., Sahl, H.-G., and Sonomoto, K. (2012) Ring A of Nukacin ISK-1: A lipid II-binding motif for type-A(II) lantibiotic. *J. Am. Chem. Soc.* 134, 3687–3690.

(20) Yin, N., Marshall, R. L., Matheson, S., and Savage, P. B. (2003) Synthesis of lipid A derivatives and their interactions with polymyxin B and polymyxin B nonapeptide. *J. Am. Chem. Soc.* 125, 2426–2435.

(21) Martin, N. I., Hu, H., Moake, M. M., Churey, J. J., Whittal, R., Worobo, R. W., and Vederas, J. C. (2003) Isolation, structural characterization, and properties of mactacin (polymyxin M), a cyclic peptide antibiotic produced by *Paenibacillus kobensis* M. *J. Biol. Chem.* 278, 13124–13132.

(22) Velkov, T., Soon, R. L., Chong, P. L., Huang, J. X., Cooper, M. A., Azad, M. A., Baker, M. A., Thompson, P. E., Roberts, K., Nation, R. L., Clements, A., Strugnell, R. A., and Li, J. (2013) Molecular basis for the increased polymyxin susceptibility of *Klebsiella pneumoniae* strains with under-acylated lipid A. *Innate Immun.* 19, 265–277.